The Receptive Endometrial Transcriptomic Signature Indicates an Earlier Shift from Proliferation to Metabolism at Early Diestrus in the Cow

Author(s): F.S. Mesquita, R.S. Ramos, G. Pugliesi, S.C.S. Andrade, V. Van Hoeck, A. Langbeen, M.L. Oliveira, A.M. Gonella-Diaza, G. Gasparin, H. Fukumasu, L.H. Pulz, C.M. Membrive, L.L. Coutinho, and M. Binelli

Source: Biology of Reproduction, 93(2)
Published By: Society for the Study of Reproduction
URL: http://www.bioone.org/doi/full/10.1095/biolreprod.115.129031

BIOLOGY OF REPRODUCTION (2015) **93**(2):52, 1–12
Published online before print 15 July 2015.
DOI 10.1095/biolreprod.115.129031

The Receptive Endometrial Transcriptomic Signature Indicates an Earlier Shift from Proliferation to Metabolism at Early Diestrus in the Cow[1]

F.S. Mesquita,[3,4] R.S. Ramos,[3,5] G. Pugliesi,[5] S.C.S. Andrade,[5,6] V. Van Hoeck,[5] A. Langbeen,[9] M.L. Oliveira,[5] A.M. Gonella-Diaza,[5] G. Gasparin,[6] H. Fukumasu,[7] L.H. Pulz,[7] C.M. Membrive,[8] L.L. Coutinho,[6] and M. Binelli[2,5]

[4]*Universidade Federal do Pampa, Curso de Medicina Veterinária, Uruguaiana, Rio Grande do Sul, Brazil*
[5]*Universidade de São Paulo, Faculdade de Medicina Veterinária e Zootecnia, Departamento de Reprodução Animal, Pirassununga, São Paulo, Brazil*
[6]*Universidade de São Paulo, Escola Superior de Agricultura "Luiz de Queiroz", Departamento de Zootecnia, Piracicaba, São Paulo, Brazil*
[7]*Universidade de São Paulo, Faculdade de Zootecnia e Engenharia de Alimentos, Pirassununga, São Paulo, Brazil*
[8]*Universidade Estadual Paulista "Júlio de Mesquita Filho", Campus Experimental de Dracena, Dracena, São Paulo, Brazil*
[9]*University of Antwerp, Faculty of Pharmaceutical, Biomedical and Veterinary Sciences, Wilrijk, Belgium*

ABSTRACT

This study aimed to characterize the endometrial transcriptome and functional pathways overrepresented in the endometrium of cows treated to ovulate larger (≥13 mm) versus smaller (≤12 mm) follicles. Nelore cows were presynchronized prior to receiving cloprostenol (large follicle [LF] group) or not (small follicle [SF] group), along with a progesterone (P4) device on Day (D) −10. Devices were withdrawn and cloprostenol administered 42–60 h (LF) or 30–36 h (SF) before GnRH agonist treatment (D0). Tissues were collected on D4 (experiment [Exp.] 1; n = 24) or D7 (Exp. 2; n = 60). Endometrial transcriptome was obtained by RNA-Seq, whereas proliferation and apoptosis were assessed by immunohistochemistry. Overall, LF cows developed larger follicles and corpora lutea, and produced greater amounts of estradiol (D−1, Exp. 1, SF: 0.7 ± 0.2; LF: 2.4 ± 0.2 pg/ml; D−1, Exp. 2, SF: 0.5 ± 0.1; LF: 2.3 ± 0.6 pg/ml) and P4 (D4, Exp. 1, SF: 0.8 ± 0.1; LF: 1.4 ± 0.2 ng/ml; D7, Exp. 2, SF: 2.5 ± 0.4; LF: 3.7 ± 0.4 ng/ml). Functional enrichment indicated that biosynthetic and metabolic processes were enriched in LF endometrium, whereas SF endometrium transcriptome was biased toward cell proliferation. Data also suggested reorganization of the extracellular matrix toward a proliferation-permissive phenotype in SF endometrium. LF endometrium showed an earlier onset of proliferative activity, whereas SF endometrium expressed a delayed increase in glandular epithelium proliferation. In conclusion, the periovulatory endocrine milieu regulates bovine endometrial transcriptome and seems to determine the transition from a proliferation-permissive to a biosynthetic and metabolically active endometrial phenotype, which may be associated with the preparation of an optimally receptive uterine environment.

endometrium, fertility, genomics, gonadal steroids, ruminants (cows, sheep, llama, camel)

INTRODUCTION

Although the pathway from conception to a healthy, full-term pregnancy encompasses a plethora of cellular processes taking place from early events that precede fertilization, it has been accepted that the overall fertility outcome is under a major influence of the uterine environment [1–5]. In this context, the profile of molecules of distinct biochemical natures, such as ions, vitamins, proteins/peptides (e.g., hormones, growth factors, mitogens, protease/protease inhibitors), amino acids, and carbohydrates (e.g., glucose, fructose), which are either transported or expressed and secreted by the endometrium into the uterine lumen [6], altogether contribute to the composition of the uterine luminal content, known as histotroph. Prior to the establishment of intimate interaction with the endometrial lining, the embryo relies on the trophic characteristics of the histotroph for its early development (i.e., growth and elongation), therefore influencing its ability to secrete interferon tau and block the luteolysis-triggering cascade, which is a prerequisite to sustain the ongoing pregnancy [7–9].

Due to the contemporaneous relationship between the arrival of the embryo into the uterine environment and the early, histotroph-dependent embryo growth phase and the linear increase in progesterone (P4) secretion during early diestrus, a major effort has been made to investigate the molecular profile of the endometrium in response to exposure to P4 exogenous supplementation during diestrus [3, 10]. Furthermore, it has also been demonstrated that the preovulatory endocrine profile majorly impacts endometrial characteristics expressed later during metaestrus and early diestrus, as well as embryo development and conception rates [11–17]. Whereas numerous studies have mainly focused on late diestrus for transcriptome-based endometrial mechanistic characterization, a study by Demetrio et al. [2] suggested an earlier moment for endometrial sampling and investigation of fertility-related functional relationships. Demetrio et al. [2]

[1]Supported by Fundação de Amparo à Pesquisa do Estado de São Paulo to F.M., R.R., G.P., S.C.S.A., V.V.H., and M.B.; Conselho Nacional de Desenvolvimento Científico e Tecnológico to M.B.; and Coordenação de Aperfeiçoamento de Pessoal de Nível Superior to A.M.G. Reads sequences are accessible under Gene Expression Omnibus accession number GSE65450. Presented in part at the 46th Annual Meeting of the Society for the Study of Reproduction, 22–26 July 2013, Montreál, Quebéc, Canada.
[2]Correspondence: Mario Binelli, Universidade de São Paulo, Faculdade de Medicina Veterinária e Zootecnia, Departamento de Reprodução Animal, Avenida Duque de Caxias Norte, 225, 13635-900, Pirassununga, São Paulo, Brazil. E-mail: binelli@usp.br
[3]These authors contributed equally to this work.

Received: 18 February 2015.
First decision: 24 March 2015.
Accepted: 19 June 2015.

eISSN: 1529-7268 http://www.biolreprod.org
ISSN: 0006-3363

reported that there was a positive impact of P4 concentrations measured on Day 7 postestrus on probability of conception of inseminated dairy cows, but not on conception of cows receiving an embryo by embryo transfer on Day 7 [2]. This study suggested that the in utero exposure of the embryo to the primed endometrium during the first week of pregnancy is necessary for the identification of an endocrine profile-dependent effect. It can be speculated that P4, as well as preceding estradiol (E2), are acting through the modulation of endometrial tissue phenotype to prepare an optimally receptive uterine environment to the embryo that is arriving from the oviduct.

Based on the above evidence, it is hypothesized that, during the period that encompasses the periovulatory stages (i.e., proestrus, estrus, metaestrus, and early diestrus), endometrial cell types are under the influence of sequential endocrine events, majorly characterized by follicular and luteal development, and secretion of E2 and P4, which interfere with the receptive status of the uterus [18, 19]. Although several studies have shed light on correlational relationships between the periovulatory endocrine milieus and the preparation of bovine endometrial receptivity toward the embryo, clear mechanistic insights are lacking so far. Our group explored and characterized a regime of hormonal manipulation of the estrous cycle that modulates preovulatory follicle size by anticipation of luteolysis during late follicle growth [20]. That animal model not only modulates preovulatory E2 concentrations, corpus luteum (CL) development, and diestrus P4 secretion pattern, but also impacts fertility in beef cattle [21]. Here, we report, for the first time, the impact of the sequential exposure to physiological ovarian steroids, taking place during the periovulatory phase, on endometrial transcriptional and phenotypic profiles. More specifically, this study provides previously lacking mechanistic information regarding the reported positive impact of the presented animal model on fertility in beef cattle. Specific aims of this study were: 1) to characterize the endometrial transcriptome, 2) to identify functional pathways, and 3) to molecularly characterize selected pathways overrepresented in the endometrium collected at early diestrus of cows that were treated to ovulate larger ($\geq$13 mm) versus smaller ($\leq$12 mm) follicles. It is proposed that the uterine biology, represented by the endometrial transcriptome, is differentially regulated by the periovulatory endocrine milieu. Moreover, based on the distinct E2 and P4 secretion profiles identified by Mesquita et al. [20] (i.e., timing and magnitude of E2 and P4 during proestrus and early diestrus, respectively [20]), it is expected that endometrial tissue global gene expression will distinctly represent molecular profiles that characterize endometrial cellular/tissue phenotypes expressed according to the periovulatory endocrine environment experienced.

MATERIALS AND METHODS

Animals and Reproductive Management

Animal procedures were approved by the Ethics and Animal Handling Committee of the Faculdade de Medicina Veterinária e Zootecnia, Universidade de São Paulo (CEUA-FMVZ/USP, No. 2287/2011). Experiments were carried out at the Universidade de São Paulo in Pirassununga, São Paulo, Brazil.

Experiment (Exp.) 1. Animals were kept under grazing conditions and supplemented with sugar cane and/or corn silage, concentrate, and minerals to fulfill their maintenance requirements, and water ad libitum. Nonlactating, multiparous Nelore (*Bos taurus indicus*) cyclic cows (presenting a CL), presenting no gross reproductive abnormalities by gynecological examination, aged between 4 and 10 yr, weighed 535.1 $\pm$ 60.9 kg, and had a body condition score of 3.72 $\pm$ 0.23. A total of 56 cows were presynchronized (Presynch) by two intramuscular injections of prostaglandin F2 alpha analog (PGF; 0.5 mg of sodium cloprostenol; Sincrocio, Ouro Fino, Cravinhos, Brazil), 14 days apart. At the second PGF injection of Presynch (Day [D] −20), animals were equipped with an ESTROTECT Heat detector patch (Rockway, Inc. Spring Valley, WI), and estrus detection was performed twice daily from D−19 to D−16, and once daily from D−15 to D−10. Subsequent manipulations were performed 10 days after the second PGF injection (D−10), according to the hormonal protocol indicated by Figure 1. Only animals that had a fresh, PGF-responsive CL (at least 5 days old) on D−10 stayed in the experiment; 15 cows did not responded to the Presynch protocol and were, therefore, removed from the experiment. Remaining cows (n = 41) received a new intravaginal P4-releasing device (1 g; Sincrogest, Ourofino) on D−10 along with an intramuscular injection of 2 mg estradiol benzoate (Sincrodiol, Ourofino). Simultaneously, only cows in the large follicle (LF) group received an intramuscular injection of PGF. P4-releasing devices were removed prior to GnRH injection from LF (n = 20) and the small follicle (SF; n = 21) cows. All animals received two PGF injections 6 h apart at P4 device removal. Ovulation was induced by an injection of 10 μg Buserelin on D0 (Sincroforte, Ourofino). Animals that responded to treatments as defined by design (please see the *Statistical Analysis* section) were slaughtered on D4 after induction of ovulation (n = 24).

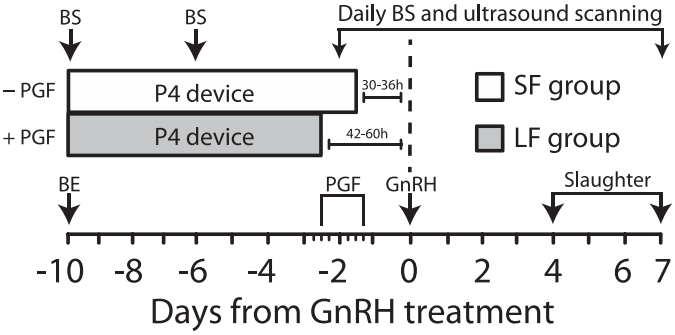

FIG. 1. Schematic of the hormonal manipulation protocol used in the present study. BE, injection of 2 mg of estradiol benzoate (Sincrodiol; Ourofino); BS, blood sampling; GnRH, injection of 0.01 mg of buserelin acetate (Sincroforte; Ourofino); P4 device, P4-releasing device containing 1 g of P4 (Sincrogest; Ourofino, Cravinhos, SP, Brazil); PGF, injection of 0.5 mg of sodium cloprostenol (Sincrocio; Ourofino); Slaughter, endpoint for endometrium collection (Exp. 1, n = 56; Exp. 2, n = 74).

Experiment 2. A total of 83, nonlactating, multiparous Nelore (*B. indicus*) cows presenting no gross reproductive abnormalities by gynecological examination were kept under grazing conditions and supplemented with sugar cane and/or corn silage, concentrate, and minerals to fulfill their maintenance requirements, and water ad libitum. Cows were cycling (with the presence of a CL), aged between 4 and 10 yr, weighed 461.6 $\pm$ 50.1 kg, and presented a body condition score of 3.67 $\pm$ 0.33. Only animals that had a fresh, PGF-responsive CL (at least 5 days old) on D−10 stayed in the experiment (eight cows had P4 $<$ 1.0 ng/ml and one was not detected in estrus, and they were, therefore, eliminated). Animals were manipulated according to the same hormonal protocol used in Exp. 1 (Fig. 1), except for the day of tissue harvesting, which took place on D7 after induction of ovulation. Of the 83 animals that were presynchronized, 39 cows were destined to compose the SF group, whereas 35 were included in the LF group. Animals that responded to treatments as defined by design (please see the *Statistical Analysis* section) were slaughtered on D7 after induction of ovulation (n = 60)

Blood Sampling and Hormone Measurements

Blood sampling for determination of P4 concentrations was performed once on D−10, D−6, and D−2, and daily from D1 to D4 (Exp. 1) or D7 (Exp. 2). Blood samples were collected by jugular venipuncture using evacuated tubes containing ethylene diamine tetra-acetic acid (EDTA; BD, São Paulo, SP, Brazil). Plasma was separated by centrifugation at 4°C, 1500 $\times$ *g* for 30 min and stored at −20°C. P4 concentrations were measured in all samples using a solid-phase radioimmunoassay (Coat-a-Count; DPC, Los Angeles, CA), as validated previously [22]. Plasma E2 concentrations were determined for D−2, D−1, and D0 using a commercial RIA kit (Double Antibody Estradiol; DPC) as reported previously [23].

Ultrasound Examinations

Transrectal ultrasound examinations to assess growth of the dominant follicle, ovulation, and CL development were carried out on D−10, daily from D-2 to D0 and from D3 to D4 (Exp. 1) or D7 (Exp. 2), and every 12 h from D1 to D2. Ultrasonography was performed with the aid of a duplex B-mode (gray scale) and pulsed-wave color Doppler ultrasound instrument (MyLab30 Vet Gold; Esaote Healthcare, São Paulo, SP, Brazil) equipped with a multifrequency linear transducer. Retrospective interpretation of changes in follicular diameters over time allowed the identification of the dominant follicle of the estradiol benzoate-induced wave, the determination of the dominant follicle preovulatory diameter, and the day of ovulation. Ovulation was defined as the disappearance of the preovulatory follicle identified previously, followed by the observation of a CL on the same approximate topographical location on the ovary. The diameter of follicles and CLs were calculated as the average between measurements of two perpendicular axes of each structure.

Tissue Processing

On D4 (Exp. 1) or D7 (Exp. 2), cows were stunned by captive bolt and killed by jugular exsanguination. Reproductive tracts were transported on ice and dissected within 15 min of slaughter. Intercaruncular endometrial tissue was dissected from the anterior, medial, and posterior regions of the uterine horn ipsilateral to the ovary containing the CL, and pooled. Pooled tissue was snap frozen and stored at −80°C for subsequent processing.

RNA Isolation and cDNA Synthesis

Approximately 30 mg of endometrial tissue was ground in liquid nitrogen using a stainless steel apparatus and immediately mixed with buffer RLT from the RNeasy Mini columns kit (Qiagen, São Paulo, SP, Brazil), per the manufacturer's instructions. To maximize lysis, tissue suspension was passed at least 10 times through a 21-G needle and centrifuged at 13 000 × *g* for 3 min for removal of debris prior to supernatant loading and processing in RNeasy columns. Columns were eluted with 40 µl of RNase-free water, and elution was repeated using the same 40 µl initially used to increase RNA concentration. Concentration of total RNA on extracts was measured by a spectrophotometer (NanoDrop; Thermo Scientific, Wilmington, DE). Prior to reverse transcription, 1 µg of total RNA was treated with DNAse I (Life Technologies, São Paulo, SP, Brazil) for 15 min at room temperature in a 10-µl reaction, followed by addition of 1 µl of EDTA (25 mM) and heating at 65°C for 10 min to inactivate DNase I. DNase I treatment was immediately followed by reverse transcription (High Capacity cDNA Reverse Transcription Kit; Life Technologies) according to the manufacturer's instructions. Briefly, 9 µl of master mix containing RT buffer, dNTP mix, random primers, RNase inhibitor, and reverse transcriptase were added to the 11 µl of DNase I treatment reaction. Samples were immediately incubated at 25°C for 10 min, followed by incubation at 37°C for 2 h, reverse transcriptase inactivation at 85°C for 5 min, and storage at −20°C.

Messenger RNA Libraries and Sequencing

Integrity of total RNA extracts was assessed using the Agilent RNA 6000 Nano chip (Bioanalyzer; Agilent Technologies; Santa Clara, CA). RNA integrity number of extracts submitted to RNA sequencing analysis ranged from 8.3 to 8.7. After that, 4 µg of RNA was used with the TruSeq RNA Sample Preparation kit (Illumina, San Diego, CA) to prepare the libraries for RNA-Seq. The insert sizes were estimated through the Agilent DNA 1000 chip (Agilent Technologies) and the library concentrations were measured through quantitative real-time PCR with a KAPA Library Quantification kit (KAPA Biosystems). Samples were diluted, pooled in equimolar amounts and then sequenced at the Centro de Genômica Funcional Aplicada à Agropecuária e Agroenergia using a HiScanSQ sequencer (Illumina).

Bioinformatics

Following sequencing, the 100-bp paired end (PE) reads were filtered using a perl script, which removed all reads with a mean quality under 26. The reads were mapped with Bowtie2 v2.1.0 [24] on the masked bovine genome assembly (*Bos taurus* UMD 3.1; http://www.ncbi.nlm.nih.gov/genome/guide/cow/index.html). The mapping file was sorted using SAMTools v 0.1.18 [25] and read counts were obtained using the script from HTSeq-count v0.5.4p2 (http://www-huber.embl.de/users/anders/HTSeq/doc/count.html [26]). The differential expression analysis was performed with package DE-SEq v1.12.1 [27], from R [28]. Using the function estimateSizeFactors, the normalized counts were obtained (baseMean values, which are the number of reads divided by the size factor or normalization constant). The standard deviation along the baseMean values was also calculated for each transcript. In order to avoid artifacts caused by low expression profiles and high expression variance, only transcripts that had an average of baseMean > 5 and the mean greater than the standard variation were analyzed. The threshold for evaluating significance was obtained by applying a P value of 0.05 false discovery rate Benjamini-Hochberg [29]. Integrated analysis of different functional databases was done using the functional annotation tool of the Database for Annotation, Visualization, and Integrated Discovery [30] using, as background, the set of genes that passed through the differential expression analysis filter.

Immunohistochemistry for MKI67

Paraffin-embedded endometrial samples (Exp. 1, SF, n = 5, LF, n = 6; Exp. 2, SF, n = 4, LF, n = 5) were stained with antibodies against MKI67 to determine the proportion of proliferating cells. Tissue sections, 4 µm thick, were deparaffinized in xylene and rehydrated in an ethanol series. Sections were then subjected to antigen retrieval by pressure cooking in citrate buffer (10 mM citric acid, 0.05% Tween 20, pH 6.0), preheated to 80°C, for 1 min. Tissue sections were allowed to cool for 20 min and rinsed with 1× PBS (1.09 g of Na_2HPO_4 anhydrous, 0.32 g of NaH_2PO_4 anhydrous, 9 g of NaCl, 1000 ml of distilled water, pH 7.4). The incubation with monoclonal mouse anti-human MKI67 primary antibody, Clone MIB-1 (code M7240; DAKO, Denmark) was performed in diluted PBS (1:76, which corresponds to 0.45 µg/ml), overnight at 4°C. Negative control slides were incubated with normal mouse IgG (sc-2025; Santa Cruz Biotechnology, Santa Cruz, CA) at the same concentration of the primary antibody. Both incubations were performed overnight at 4°C. After the wash series, slides were incubated with UltraVision ONE Detection System: HRP Polymer (TL-015-HDJ; Thermo Scientific, Waltham, MA) for 30 min at room temperature. After washing, 3,3-diaminobenzidine tetrahydrochloride (K3468; Dako, Carpinteria, CA) was used as chromogen. The sections were counterstained lightly with hematoxylin, dehydrated, cleared in xylene, and mounted on cover slips. Immunohistochemical images were captured by Zeiss Axioplan 2 microscope imaging analysis system (Carl Zeiss, Göttingen, Germany). Only those tissues containing cells with a distinct nuclear staining for MKI67 were considered to be positive.

IHC for Activated CASP3

Paraffin embedded endometrial samples (n = 6/group) were stained with antibodies against activated CASP3 to determine the number of positive apoptotic cells. The immunohistochemical procedures were performed in collaboration with the Gamete Research Centre, University of Antwerp. Tissue sections were deparaffinized in xylene and rehydrated in an ethanol series. After rehydration, sections were pretreated in an antigen retrieval citrate solution. Pretreatment consisted of microwaving the slides for 20 min at 90 W, cooling down for 20 min at room temperature, and incubating slides for 5 min with 3% hydrogen peroxide solution. Slides were then rinsed in Tris-buffered saline (TBS; 0.5M Tris base, 9% NaCl, pH 8.4) and tissue sections subsequently covered with 50 µl of normal goat serum and incubated for 20 min at room temperature in order to prevent nonspecific signal. The immunohistochemical detection of activated CASP3 was performed using a polyclonal rabbit anti-activated CASP3 antibody raised against human and mouse activated CASP3 (C8487, Sigma), which cross-reacts with the bovine protein. All sections were incubated overnight at room temperature with 50 µl of a 1-µg/ml concentrated primary rabbit antibody. Sections were rinsed in TBS and incubated for 30 min at room temperature with anti-rabbit immunoglobulin conjugated with peroxidase (K4003; Dako; Denmark). Finally, after rinsing in PBS, 50 µl of diaminobenzidine chromogenic substrate was added and incubated for 5 min. Hematoxylin counterstaining was carried out for 30 sec. Negative controls were included in every staining procedure, and corresponded to uterine tissue sections incubated with PBS instead of the primary anti-activated CASP3 antibody.

Statistical Analysis

According to Mesquita et al. [20], by design, animals were excluded from data analyses if: P4 concentration on D−10 was less than 1 ng/ml, P4 concentration on D−2 was greater than 3 ng/ml in the LF group, P4 concentration on D−2 was less than 2 ng/ml in the SF group, dominant follicle diameter on D0 was less than 8 mm, ovulation was detected at the D0 ultrasound examination or before (i.e., early ovulation), ovulation was detected at the D3 ultrasound examination (i.e., late ovulation), ovulation was not detected, or follicular, or luteal cysts or lesions impairing animal well being were detected at any moment during the experiment. Nonnormally distributed data from dependent variables according to the Shapiro-Wilk test were transformed to natural logarithms or ranks. Follicle diameter, P4 concentra-

TABLE 1. Follicle, CL, E2, and P4 measurements of cows from experiments 1 and 2, ovulating within the first 48 h post-GnRH.

	Exp. 1[a]			Exp. 2[a]		
End point	SF (n = 8)	LF (n = 8)	*P* value	SF (n = 11)	LF (n = 7)	*P* value
Follicle diameter (mm)[b]	11.31 ± 0.23	15.70 ± 0.43	<0.01	10.63 ± 0.30	13.18 ± 0.44	< 0.01
Plasma E2 concentrations on D-1 (pg/ml)[c]	0.65 ± 0.15	2.44 ± 0.19	<0.01	0.50 ± 0.13	2.30 ± 0.57	< 0.01
CL volume (mm^3)	2.31 ± 0.10[d]	2.53 ± 0.09[d]	0.06	1.80 ± 0.19[e]	2.91 ± 0.54[e]	0.04
Plasma P4 concentrations (ng/ml)[f]	0.80 ± 0.10	1.40 ± 0.23	<0.01	2.49 ± 0.43	3.68 ± 0.38	0.04

[a] Values are expressed as means ± SEM.
[b] D–1 in Exp. 1; D0 in Exp. 2.
[c] E2 concentrations were assayed in a subset of animals (n = 5–6/group).
[d] Measured by ultrasonography.
[e] Measured postmortem.
[f] D4 in Exp. 1; D7 in Exp. 2.

tions, and CL volume were analyzed using split-plot ANOVA, including the effects of group, day, and interaction. The MIXED procedure (PROC MIXED, SAS, version 9.2; SAS Institute Inc., Cary, NC) was used with a REPEATED statement to account for autocorrelation between sequential measurements, including cow within group as a random variable. Discrete dependent variables were analyzed using one-way ANOVA for the effect of group using the general linear model procedure (SAS). A probability of $P \leq 0.05$ indicated that a difference was significant, and a probability of $P > 0.05$ to $P \leq 0.1$ indicated a tendency. Data are presented as the mean ± SEM, unless otherwise indicated. Poisson regression was used for IHC data (MKI67 and activated CASP3) analysis. Positive versus negative cells were compared between LF and SF by chi-square test (PROC FREQ; SAS). Generalized linear model with Poisson distribution (PROC GLIMMIX; SAS) was used when there was statistical significance ($P < 0.05$) in the chi-square for each variable.

RESULTS

Ovarian and Endocrine Variables

Animals manipulated to ovulate follicles at distinctly different sizes presented contrasting ovarian morphology and sex steroid endocrine profiles. In Exp. 1, cows from the LF group developed larger follicles (1.4 times) and CLs (1.4 times), and produced greater amounts of E2 (3.8 times) and P4 (1.8 times) (Table 1). Similarly, LF animals developed larger (1.6 times) CLs and reached plasma P4 concentrations 1.5 times greater than SF animals. In Exp. 2, follicle diameter and plasma E2 concentrations were 1.2 and 2.3 times greater in the LF group than in the SF group, as demonstrated in Table 1. A more comprehensive description of the animal model used in this study was published previously [20].

RNA-Seq

Three biological replicates from Exp. 2 were analyzed for each experimental group, and RNA sequencing produced a total of approximately 134 million reads with an average of 22 million reads for each sample. All read sequences were deposited in the Sequence Read Archive (SRA) of the National Center for Biotechnology Information (NCBI; http://www.ncbi.nlm.nih.gov/sra/ [31]; accession number in Supplemental Table S1; supplemental data are available online at www.biolreprod.org), and an overview of these data has been deposited in NCBI's Gene Expression Omnibus (GEO) and is accessible through GEO Series accession number GSE65450. Reads ranged from 14 to 39 million per sample after filtering. The numbers of reads used and mapped are presented in Supplemental Table S2. Approximately 62% of the total reads uniquely mapped to the UMD 3.1 reference genome. There were approximately 10% of reads that were not-uniquely mapped, 15% nonspecifically mapped reads, and 20% unmapped reads. Only the uniquely mapped reads were considered in the analysis.

To categorize the genes with different levels of expression, a multiphasic graph was obtained by plotting the log2-transformed read values (baseMean) versus all expressed genes from the *B. taurus* genome (24 616). According to the phases in the graph, gene expression values were categorized into three groups: high (≥1000 normalized reads), medium (15–1000 normalized reads), and low (<15 normalized reads) expression genes. There were 2272 (9.3%) genes with high expression, 11 450 (46.5%) genes with medium expression, and 10 894 genes (44.2%) with low expression. There were 2209 (8.9%) and 2318 (9.5%) highly expressed genes in SF and LF, and 10 907 (44.3%) and 11 006 (44.7%) lowly expressed genes in SF and LF, respectively.

After applying the filter for variance and minimal value of baseMean, a total of 14 540 genes were included on the differential expression analysis. A total of 562 genes showed differential expression (adjusted *P* value < 0.1), of which 364 and 198 were upregulated in the endometrium of LF and SF animals, respectively. Differentially expressed genes (adjusted *P* value < 0.1) are listed on Supplemental Table S3 along with their respective mean normalized baseMean values per group, Log2 fold changes, and adjusted *P* values. The distance heatmap indicates the correlation among biological samples within group and distinct profile between groups (Fig. 2A). The top 10 transcripts with the highest expression values were *COL3A1* (collagen type III, alpha 1), *COL1A2* (collagen type I, alpha 2), *DCN* (decorin), *COL1A1* (collagen type I, alpha 2), *HSPA8* (heat shock 70-kDa protein 8), *ACTG1* (actin, gamma 1), *SPARC* (secreted protein, acidic, cysteine-rich; osteonectin), *OGDH* (oxoglutarate [alpha-ketoglutarate] dehydrogenase [lipoamide]), *EEF2* (eukaryotic translation elongation factor 2), and *COL6A1* (collagen, type VI, alpha 1).

Functional Enrichment Analysis of RNA-Seq Data

A total of 15 gene ontology (GO) terms were enriched in the LF group, whereas 56 were enriched in the SF group (adjusted *P* value < 0.1). From the 14 450 identified genes, 403 were assigned to biological processes, 692 to cellular components, and 336 to molecular functions for the SF-derived samples, whereas, for LF-derived samples, 273, 213, and 330 were assigned biological processes, cellular components, and molecular functions, respectively. Detailed verification of overrepresented ontology terms indicated that, in SF endometrial samples (Table 2), intracellular machinery and cellular microenvironment are mobilized toward the reorganization of non-membrane-associated organelles (e.g., cytoskeleton), activity of structural molecules and binding proteins (e.g., carbohydrates, calcium, collagen, and enzymatic inhibition), and activation of pathways associated with extracellular matrix

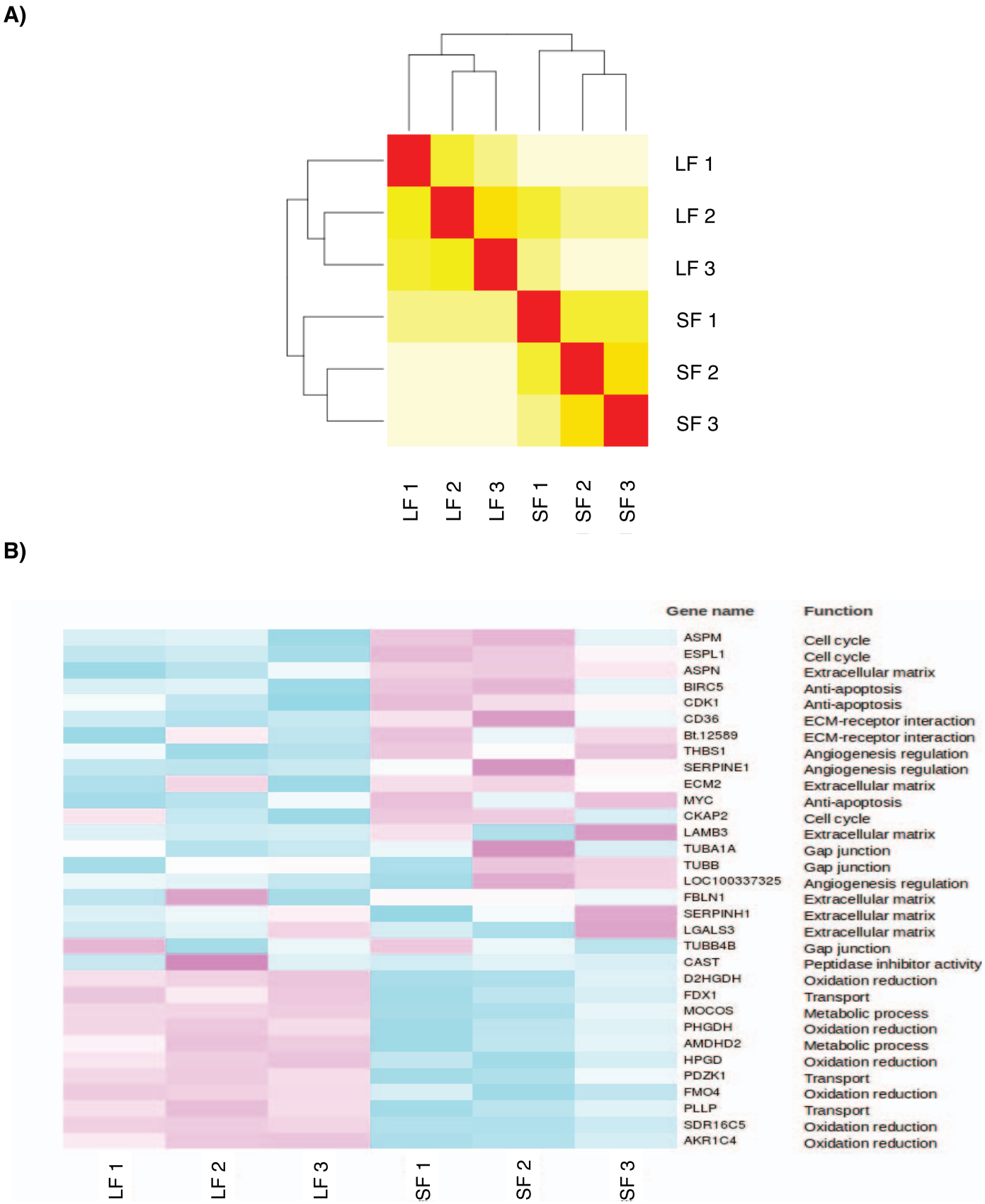

FIG. 2. Heatmaps of transcriptome data. **A**) Heatmap showing the Euclidean distances between the samples as calculated from the variance-stabilizing transformation of the count data. Each column represents one sample and shows the correlation to all samples with red for the lowest (0) distance and light yellow for the highest observed distance. Normalized count values were used. **B**) Heatmap of the expression profile of genes belonging to specific enriched gene ontologies and their respective functional annotation. Pink indicates high expression profile and dark blue the lowest expression. Normalized count values were used.

TABLE 2. Functional enrichment of genes upregulated in the endometrium of SF cows.

Ontology source	Ontology term	Gene count	Fold enrichment	*P* value[a]
Biological process	Cell cycle	12	4.83	0.000
Biological process	Cell cycle phase	9	7.03	0.000
Biological process	Cell cycle process	10	5.92	0.000
Biological process	M phase	8	7.96	0.000
Biological process	M phase of mitotic cell cycle	7	8.57	0.000
Biological process	Cellular component organization	20	2.29	0.001
Biological process	Mitotic cell cycle	7	6.28	0.001
Biological process	Microtubule-based process	7	6.22	0.001
Biological process	Nuclear division	6	7.66	0.001
Biological process	Mitosis	6	7.66	0.001
Biological process	Organelle fission	6	7.15	0.001
Biological process	Extracellular matrix organization	5	9.64	0.002
Biological process	Microtubule-based movement	5	9.44	0.002
Biological process	Extracellular structure organization	5	8.09	0.003
Biological process	Peptide cross-linking	3	30.20	0.004
Biological process	Microtubule cytoskeleton organization	4	7.40	0.016
Biological process	Regulation of angiogenesis	3	14.30	0.018
Biological process	Protein polymerization	3	14.30	0.018
Biological process	Chromosome segregation	3	11.32	0.028
Biological process	Developmental process	16	1.76	0.028
Biological process	Organelle organization	11	2.10	0.031
Biological process	Cellular protein complex assembly	4	5.25	0.039
Cell component	Extracellular region	23	4.21	0.000
Cell component	Cytoskeletal part	17	5.48	0.000
Cell component	Extracellular region part	16	5.24	0.000
Cell component	Extracellular matrix	12	7.65	0.000
Cell component	Cytoskeleton	19	4.03	0.000
Cell component	Proteinaceous extracellular matrix	11	7.85	0.000
Cell component	Microtubule cytoskeleton	12	5.39	0.000
Cell component	Non-membrane-bounded organelle	24	2.37	0.000
Cell component	Intracellular non-membrane-bounded organelle	24	2.37	0.000
Cell component	Microtubule	7	6.88	0.000
Cell component	Extracellular matrix part	5	9.28	0.002
Cell component	Spindle	5	7.46	0.004
Cell component	Endoplasmic reticulum lumen	4	11.14	0.005
Cell component	Intracellular organelle part	27	1.53	0.016
Cell component	Organelle part	27	1.52	0.017
Cell component	Intermediate filament	3	13.92	0.019
Cell component	Intermediate filament cytoskeleton	3	13.92	0.019
Cell component	Protein complex	19	1.72	0.019
Cell component	Extracellular space	6	3.68	0.022
Cell component	Centrosome	4	5.22	0.039
Cell component	Endoplasmic reticulum part	5	3.73	0.043
Cell component	Macromolecular complex	22	1.49	0.045
Molecular function	Structural molecule activity	13	5.40	0.000
Molecular function	Endopeptidase inhibitor activity	5	10.17	0.001
Molecular function	Enzyme inhibitor activity	6	6.91	0.002
Molecular function	Peptidase inhibitor activity	5	9.38	0.002
Molecular function	Protein binding	44	1.32	0.012
Molecular function	Carbohydrate binding	5	5.09	0.016
Molecular function	Calcium ion binding	9	2.65	0.018
Molecular function	Collagen V binding	2	95.63	0.021
Molecular function	Serine-type endopeptidase inhibitor activity	3	9.56	0.038
Molecular function	Molybdenum ion binding	2	38.25	0.051
KEGG pathway	ECM-receptor interaction	6	7.25	0.001
KEGG pathway	Gap junction	4	5.16	0.039
KEGG pathway	Cell cycle	5	3.52	0.048

[a] *P* represents nonadjusted probabilities.

(ECM)-receptor interactions and progression of cell cycle. On the other hand, endometrial samples of the LF group (Table 3) showed a molecular profile associated with organelle membrane components (e.g., Golgi, mitochondria, vacuoles), catalytic activity (e.g., oxidation and reduction), and activation of biosynthetic and transport processes, as well as pathways involving metabolism of biomolecules (amino acids and lipids). Figure 2B illustrates the expression profile of genes representing selected GO terms. In addition, although not identified as an overrepresented ontology term, 17 solute carrier proteins were upregulated in the LF endometrium; namely: *SLC45A2*, *SLC7A8*, *SLC31A2*, *SLC5A6*, *SLC6A14*, *SLC7A4*, *SLC13A5*, *SLC38A1*, *SLC1A4*, *SLC19A2*, *SLC16A11*, *SLC45A4*, *SLC16A13*, *SLC17A5*, *SLC44A2*, *SLC7A7*, and *SLC39A14*.

Endometrial IHC Staining for MKI67 on D4 and D7

IHC of D4 endometrial tissue (Exp. 1) revealed that LF cows presented higher proliferative activity in luminal epithelium, glandular epithelium, and stroma in comparison to SF samples, as indicated by MKI67 staining (Fig. 3 and

TABLE 3. Functional enrichment of genes upregulated in the endometrium of LF cows.

Ontology source	Ontology term	Gene count	Fold enrichment	*P* value[a]
Biological process	Oxidation reduction	19	3.09	0.000
Biological process	Carboxylic acid transport	5	7.95	0.003
Biological process	Organic acid transport	5	7.95	0.003
Biological process	Amine metabolic process	9	3.05	0.009
Biological process	Cellular amine metabolic process	8	3.18	0.012
Biological process	Nitrogen compound biosynthetic process	9	2.83	0.013
Biological process	Cofactor biosynthetic process	5	5.30	0.014
Biological process	Amine transport	4	7.39	0.016
Biological process	Monocarboxylic acid transport	3	14.32	0.017
Biological process	Cellular amino acid and derivative metabolic process	8	2.76	0.024
Biological process	Amine biosynthetic process	4	5.73	0.031
Biological process	Coenzyme biosynthetic process	4	5.59	0.033
Biological process	Autophagy	3	10.11	0.034
Biological process	Metabolic process	68	1.17	0.035
Biological process	Carboxylic acid metabolic process	10	2.19	0.037
Biological process	Oxoacid metabolic process	10	2.19	0.037
Biological process	Organic acid metabolic process	10	2.18	0.038
Biological process	Vacuole organization	3	9.04	0.042
Biological process	Cellular ketone metabolic process	10	2.11	0.045
Cell component	Membrane	54	1.38	0.002
Cell component	Autophagic vacuole	3	27.30	0.005
Cell component	Organelle membrane	16	2.20	0.005
Cell component	Vacuole	6	3.98	0.016
Cell component	Trans-Golgi network	3	12.74	0.022
Cell component	Membrane part	41	1.32	0.029
Cell component	Cytoplasmic part	40	1.32	0.032
Cell component	Mitochondrion	17	1.72	0.032
Molecular function	Cofactor binding	13	4.76	0.000
Molecular function	Coenzyme binding	10	5.00	0.000
Molecular function	Oxidoreductase activity	18	2.62	0.000
Molecular function	Catalytic activity	69	1.37	0.001
Molecular function	FAD binding	6	7.82	0.001
Molecular function	Vitamin binding	6	4.80	0.008
Molecular function	Oxidoreductase activity, acting on CH-OH group of donors	5	4.52	0.024
Molecular function	NADP or NADPH binding	3	9.89	0.036
KEGG pathway	Glycerolipid metabolism	5	8.66	0.002
KEGG pathway	Arginine and proline metabolism	5	7.02	0.005
KEGG pathway	Glycine, serine and threonine metabolism	4	8.66	0.010
KEGG pathway	Lysosome	6	3.12	0.039

[a] *P* represents nonadjusted probabilities.

Table 4). On the other hand, IHC of D7 endometrial tissue (Exp. 2) revealed that MKI67-positive cells (Fig. 4 and Table 4) in the luminal epithelium were 4.1 times more abundant in SF endometrial tissue than in LF samples. In the glandular epithelium, despite the greater number of MKI67-positive cells in LF endometrium in comparison to the SF group (1.4 times), positive cell counts in both groups represented no more than 5.5% of total cells investigated. No proliferation was observed in the stroma compartment (Fig. 4 and Table 4).

Endometrial IHC Staining for Activated CASP3 on D7

IHC for the apoptosis marker, activated CASP3 (Fig. 5), revealed that glandular epithelium from LF endometrial tissue displayed a 2.6 times greater percentage of apoptotic cells in comparison to the glandular epithelium of the SF endometrial tissue (31% vs. 12%; $P < 0.0001$; Exp. 2). In the luminal epithelium and the stromal compartments, CASP3-positive cells were rare and the number of apoptotic cells did not differ between experimental groups.

DISCUSSION

Endocrine events that immediately precede and follow ovulation drive the endometrial tissue toward the receptive state during early diestrus [12, 21, 32, 33]. In the present study, we manipulated the size of the preovulatory follicle, and therefore the periovulatory concentrations of E2 and P4 [21, 34] in order to gain mechanistic insights characterizing the endometrial transcriptomic signature in response to distinct periovulatory endocrine environment. The most relevant observations from this study are: 1) D7 bovine endometrial transcriptional profile is regulated by the periovulatory endocrine milieu; 2) ontology terms overrepresented by SF and LF upregulated genes on D7 suggest the expression of proliferative and synthetic tissue phenotypes, respectively; and 3) immunolocalization of protein markers corroborates transcriptomic data, revealing an earlier onset of proliferative activity and suggesting a phenotype switch of the endometrial tissue of cows treated to ovulate larger ($\geq$13 mm) follicles in response to the periovulatory endocrine milieu.

In the field of uterine biology, a number of studies have been carried out to characterize the endometrial molecular profile of ruminants during diestrus. P4 exogenous supplementation of either intact (pregnant versus nonpregnant) or ovariectomized animals, or suppression of plasma P4 concentrations, within the first 2 wk postestrus, have been used as tools to identify key molecules regulated by this ovarian steroid hormone [9, 10, 35–37]. The present study approached a similar question employing a model developed to improve conception rates in *B. taurus indicus* beef cattle. The model uses hormonal manipulation to modulate follicle growth and maximum diameter of the dominant preovulatory follicle, and

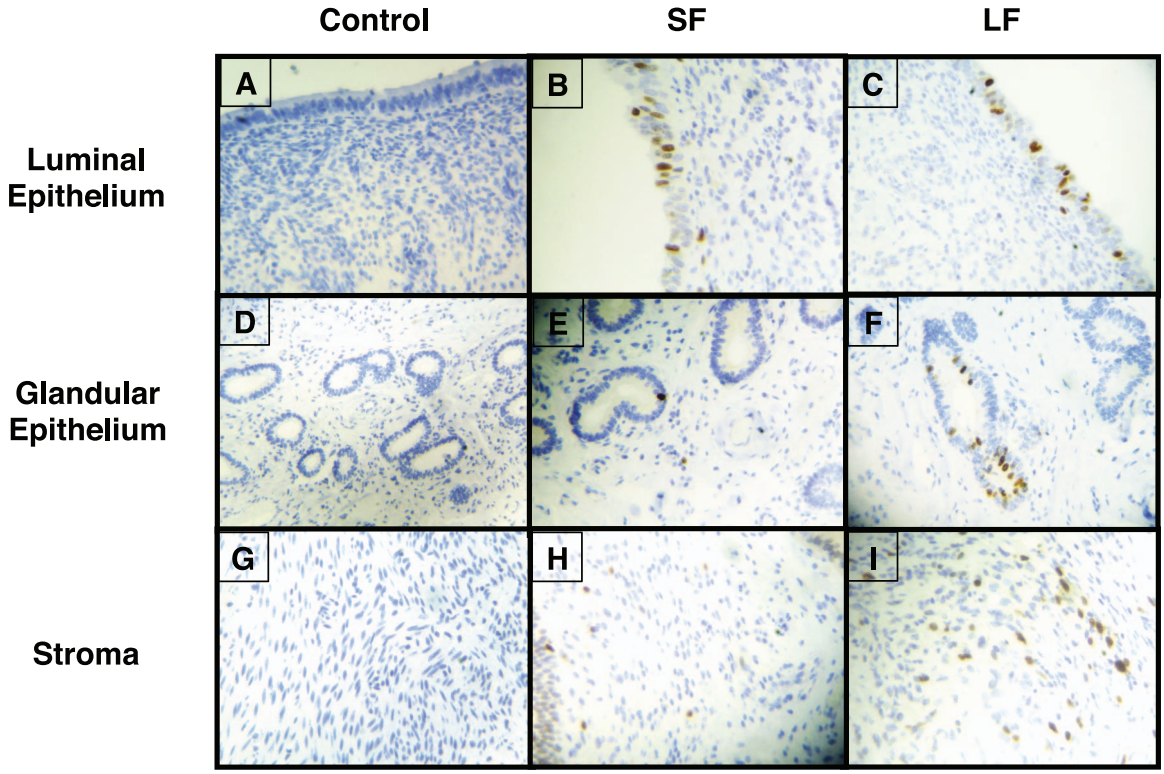

FIG. 3. Endometrial expression of MKI67 protein on D4. Protein identification by IHC on luminal epithelium (**A**–**C**), glandular epithelium (**D**–**F**), and stroma (**G**–**I**) in SF (**B**, **E**, **H**) and LF (**C**, **F**, **I**) groups. Tissue sections incubated without primary anti-MKI67 protein served as negative control group (**A**, **D**, **G**). All images were captured under 400× magnification.

has been positively associated with conception rates [21]. Most importantly, this model allowed the comparison of two distinct periovulatory endocrine environments, which varied according to the plasma E2 and P4 concentrations, during proestrus/estrus and early diestrus, respectively [20]. Our results corroborate previous reports by showing differential profiles of global gene expression between distinct endocrine environments [35, 38, 39]. Based on functional enrichment data, the observation of potentially correlated ontology terms within groups revealed an overall trend of upregulated SF endometrial genes toward cellular activities involved with cell division, ECM organization, ECM-cell interaction, and microtubule-dependent activity (e.g., mitosis). On the other hand, upregulated genes in the LF endometrium seemed to favor cellular processes associated with catalytic activity (e.g., oxidation/reduction), biosynthesis, transport, and metabolism of molecules, and organelle-related processes (e.g., vacuole, trans-Golgi network, and mitochondrion). Taken together, these findings suggest that the endometrial tissue of D7 after GnRH-induced ovulation, when exposed to distinct periovulatory endocrine environments, assumes equally distinct tissue phenotypes. Overall enrichment of proliferation and oxidation-related genes in high and low receptive bovine endometrium, respectively, have also been observed on Days 3 and 7 of the estrous cycle [40]. Similar

TABLE 4. Quantification of MKI67-positive cells identified by immunohistochemistry of formalin-fixed endometrial fragments on D4 and D7 after induction of ovulation.

	D4			D7		
Endometrial compartment	SF (5)[a]	LF (6)[a]	*P* value	SF (4)[a]	LF (5)[a]	*P* value
Luminal epithelium (500)[b]	62.6 (12.5)[e]	192 (38.4)[e]	<0.01	145.7 (29.1)[e]	35.2 (7.0)[e]	<0.01
Score 1	8	102.5	<0.01	33.3	0.4	<0.01
Score 2	54.6	89.5	<0.01	112.3	34.8	<0.01
Glandular epithelium (1000)[b]	57.4 (5.7)[e]	335.8 (33.6)	<0.01	36.7 (3.7)[e]	52.6 (5.3)[e]	0.01
Score 1[c]	5.2	164	<0.01	10.7	27.6	<0.01
Score 2[d]	52.2	171.8	<0.01	26	25	0.78
Stroma (1000)[b]	91 (9.1)[e]	255 (25.5)[e]	<0.01	Absent	Absent	
Score 1	6.6	88.5	<0.01			
Score 2	84.4	166.5	<0.01			

[a] Number of animals per group.
[b] Parentheses indicate total number of counted cells per animal.
[c] Score 1 indicates strongly stained cells.
[d] Score 2 indicates weakly stained cells.
[e] Parentheses indicate mean percentage of positive cells.

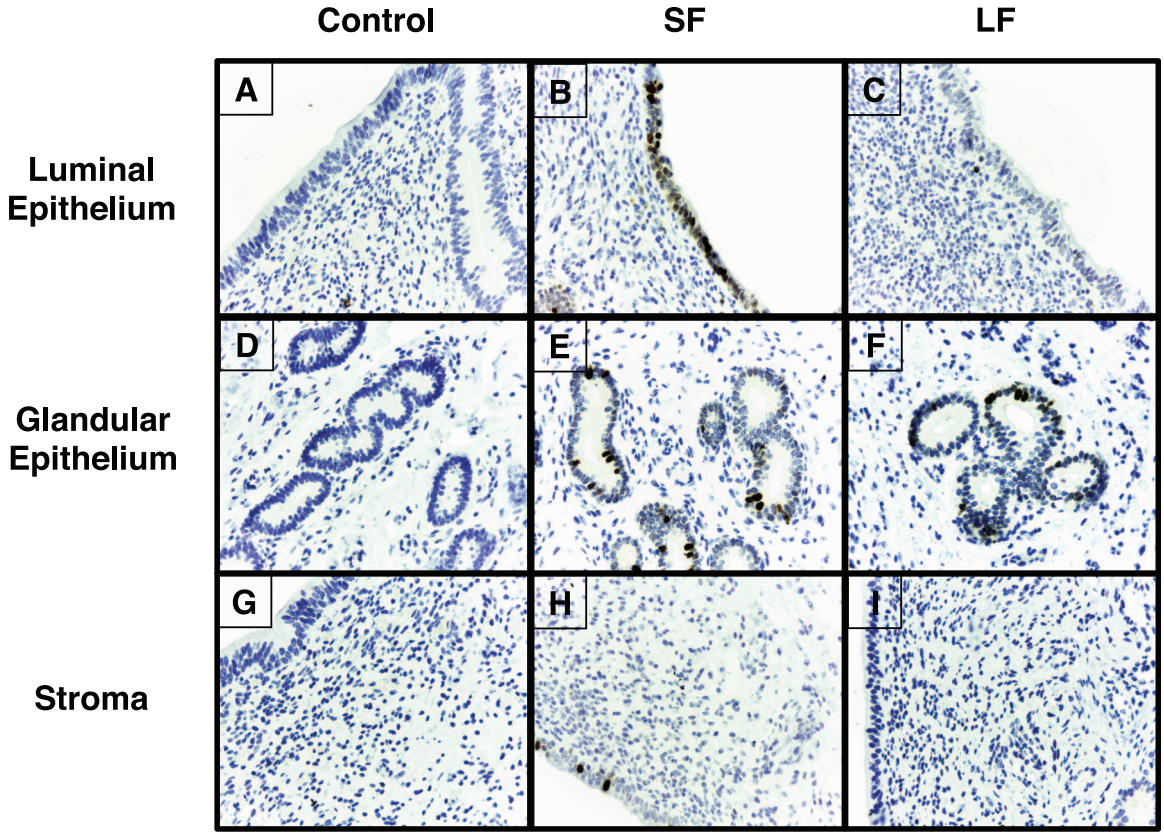

FIG. 4. Endometrial expression of MKI67 protein on D7. Protein identification by IHC on luminal epithelium (**A**–**C**), glandular epithelium (**D**–**F**), and stroma (**G**–**I**) in SF (**B**, **E**, **H**) and LF (**C**, **F**, **I**) groups. Tissue sections incubated without primary anti-MKI67 protein served as negative control group (**A**, **D**, **G**). All images were captured under 400× magnification.

functional enrichment results were observed by Minten et al. [41], who reported that Day 14 endometrial gene expression of high-fertility crossbred heifers favored transcripts associated with oxidation/reduction, cellular protein metabolic process, and ATPase activity in comparison to infertile heifers. Moreover, higher-fertility heifers showed downregulation of transcripts involved with cell cycle, response to hormone, and positive regulation of cellular differentiation [41]. Other reports, including our group's recent study, have shown that the transcript abundance of transporters (e.g., SLC solute carrier proteins) in the bovine endometrium on D7 of the estrous cycle is regulated by the periovulatory endocrine milieu [37, 42, 43] and is differentially expressed between high- and low-fertility heifers [44]. In agreement with the current literature, the present study identified 17 solute carrier proteins upregulated in the endometrial tissue of LF cows. In spite of temporal differences of endometrial sampling and animal models, the transcriptomic profile and enriched ontology terms of experiments comparing higher- to lower-fertility conditions are suggestive of very distinct tissue phenotypes (i.e., metabolism, biosynthesis, and secretion vs. proliferation). Moreover, in agreement with current literature [39], our data further support the regulation of endometrial tissue phenotype according to the timing and amplitude of exposure to distinct endocrine milieus. More specifically, it is proposed that endometrial tissue exposed earlier to higher concentrations of E2 and P4 anticipated the cellular and molecular events triggered by ovarian steroid exposure.

The nature of the ovarian steroidal endocrine profile throughout the estrous cycle regulates cellular and molecular events, including the control of endometrial tissue hyperplasia through proliferation- and apoptosis-mediated mechanisms. Investigation of the temporal and spatial fluctuations on the endometrial MKI67 and activated CASP3 signal during the bovine estrous cycle indicated higher proliferation rates during the follicular and early luteal stage (i.e., D19–D3 of the estrous cycle), associated with higher apoptosis of luminal epithelium and stroma cells [45]. In agreement with the study by Arai et al. [45], our data indicate that the LF endometrium, which was exposed earlier to increasing E2 and P4 concentrations, expressed higher proliferative activity than SF tissue on D4. Despite lack of statistical support, due to the noncontemporaneous nature of Exps. 1 and 2, over time, descriptive analysis of IHC data indicated a marked switch in the proliferation profile. Likely due to a distinct endocrine profile (i.e., delayed secretion curve of ovarian steroid with lower amplitude), overall higher proliferative activity was only expressed later, on D7, by the SF endometrial luminal epithelium compartment. In addition, our transcriptomic data also pointed to the induction of mitosis and cell cycle-related genes by the periovulatory endocrine milieu of the SF group on D7, corroborating studies that identified, on the endometrium of high-fertility heifers, a transcriptional profile associated with higher proliferative activity on D7 and lower proliferative activity on D14 in comparison to heifers of lower fertility [41, 44]. Current evidence suggests an association between timing of expression of proliferation-related transcripts by endometrial cells and fertility-associated animal models. Such speculation is supported by earlier work reporting the positive impact of an early rise in postovulatory P4 concentrations on embryo growth, development, and IFN-t production [9, 35, 46, 47].

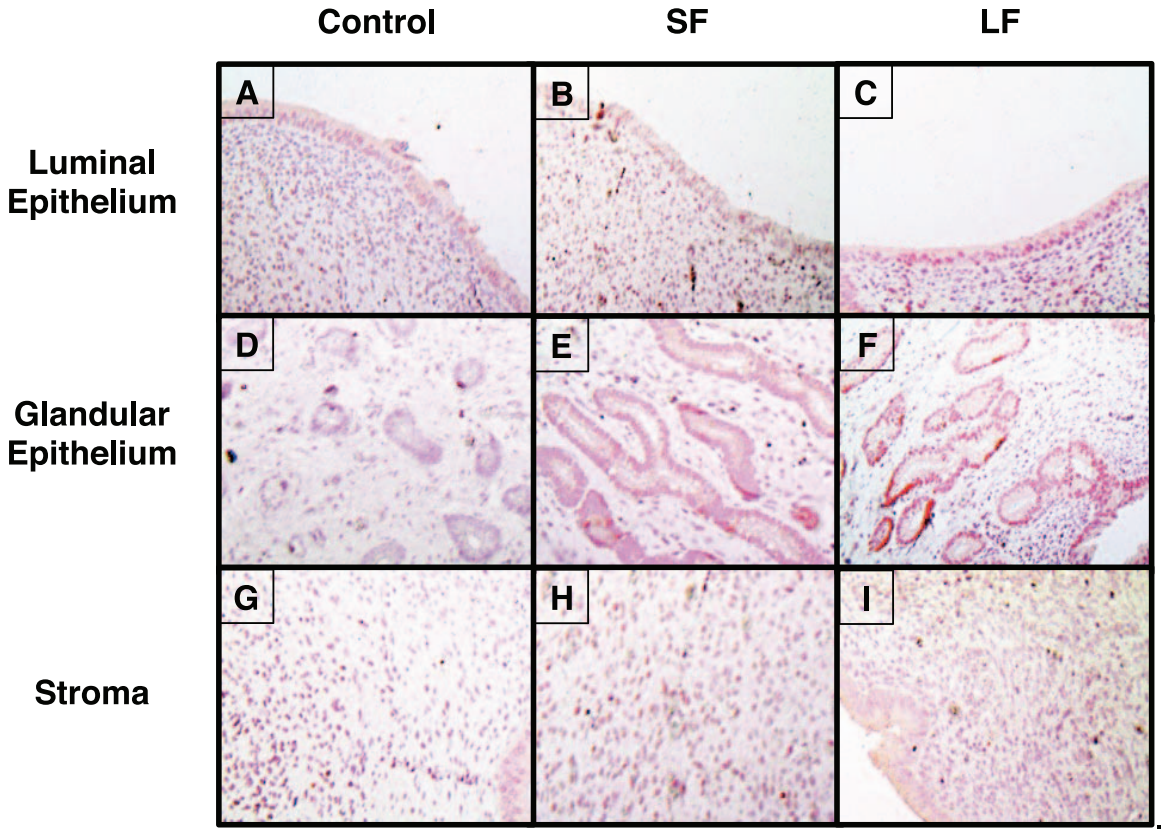

FIG. 5. Endometrial expression of activated CASP3 protein on D7. Protein identification by IHC on luminal epithelium (**A**–**C**), glandular epithelium (**D**–**F**), and stroma (**G**–**I**) in SF (**B**, **E**, **H**) and LF (**C**, **F**, **I**) groups. Tissue sections incubated without primary anti-activated CASP3 protein served as negative control group (**A**, **D**, **G**). Images in **A** through **F** were captured under 400× magnification. Images in **G** through **I** were captured under 100× magnification.

Further analysis of the functional enrichment data pointed toward genes associated with ECM composition and remodeling as major mechanistic players of the endometrial compartment. Regulation of the ECM composition represents an important mechanism by which local cues signal to the cells that different activities are required [48]. Analysis of the top 10 genes with the highest expression values revealed molecules that are directly involved with ECM organization, such as collagens and collagen-interacting proteins, indicating a differential regulation of ECM composition by distinct periovulatory endocrine milieus. Interestingly, ECM-related genes differentially expressed between experimental groups (i.e., collagens, decorin, thrombospondin, *CD36*, and tenascin C) are known to influence the organization and stability of matrix components, sequester and inhibit growth factor activity, and modulate protein synthesis and cell proliferation [49, 50]. The expression profile of matrix-related genes by the SF group is suggestive of a monomeric collagen-based ECM. Interestingly, there is solid evidence indicating that monomeric collagen is permissive to cell proliferation, whereas fibrilar collagen inhibits it [51]. Such a cellular microenvironment may provide a stable signal to the endometrial cells indicating that proliferation is no longer the target phenotype. Therefore, our data suggest an extracellular microenvironment in the SF endometrial tissue that is permissive to proliferation and less favorable to biosynthesis and metabolic exchange, which is in agreement with our functional enrichment results. However, in spite of the expected decrease in proliferative activity of luminal and glandular epithelial cells in the LF endometrial tissue from D4 to D7, glandular epithelial cells of the SF endometrium also showed a decrease (1.6 times) in MKI67-positive cells, in addition to cessation of stroma cell proliferation from D4 to D7. In that regard, a subset of genes with elevated expression in the SF endometrial tissue, such as decorin and laminins, are suggestive of an ECM composition that suppresses cell proliferation, inhibits response to growth factors, induces cell cycle arrest, and stimulates cellular differentiation [49, 50, 52, 53]. Taken together, these observations may suggest that, in spite of an overall SF endometrial tissue proliferation-permissive environment in comparison to LF tissue on D7, a subpopulation of cells, potentially the glandular epithelial compartment, seems to be undergoing the phenotype switch experienced by the LF endometrium from D4 to D7. Speculation on mechanisms based on global gene expression data provides a broad range of possibilities to explore through a rather narrow view of a universe of information that includes protein translation and degradation, protein-protein interactions, and, ultimately, protein activity. Therefore, the mechanisms proposed here, although considered appropriate and plausible, warrant further investigation.

In conclusion, the periovulatory endocrine milieu affected the D7 endometrial molecular signature. The main pathways affected were related to cell proliferation, ECM composition and remodeling, and biosynthetic and metabolic processes. Reported data further suggest that the endometrial tissue from LF cows experienced an early proliferative phase (D4), whereas the SF endometrium, exposed to a distinct periovulatory endocrine environment, expressed a delayed onset of the proliferative activity (D7). The integrated approach based on the transcriptome and phenotypic data is suggestive of a shift from a proliferation-permissive phenotype to a more biosyn-

thetic and metabolically active endometrium, which may be necessary to provide the endometrium-derived trophic factors toward the early developing embryo floating in the endometrial lumen.

ACKNOWLEDGMENT

The authors thank the administration of the Pirassununga campus of the University of São Paulo and Ourofino Saúde Animal for providing the animals and the products for pharmacological manipulation of the estrous cycle, respectively. We are also thankful to the staff of the FMVZ-USP campus Pirassununga and our laboratory colleagues, namely, Everton Lopes, Estela Araujo, Heitor Amaral, Stephanie Galindo, Moana França, Saara Scolari, Mariana Sponchiado, Bruna Miagawa, Yasmin Paiva, Fabio D'Alexandri, and Fabio Pinaffi, for animal handling and technical support, respectively.

REFERENCES

1. Salilew-Wondim D, Holker M, Rings F, Ghanem N, Ulas-Cinar M, Peippo J, Tholen E, Looft C, Schellander K, Tesfaye D. Bovine pretransfer endometrium and embryo transcriptome fingerprints as predictors of pregnancy success after embryo transfer. Physiol Genomics 2010; 42: 201–218.
2. Demetrio DG, Santos RM, Demetrio CG, Vasconcelos JL. Factors affecting conception rates following artificial insemination or embryo transfer in lactating Holstein cows. J Dairy Sci 2007; 90:5073–5082.
3. Satterfield MC, Song G, Kochan KJ, Riggs PK, Simmons RM, Elsik CG, Adelson DL, Bazer FW, Zhou H, Spencer TE. Discovery of candidate genes and pathways in the endometrium regulating ovine blastocyst growth and conceptus elongation. Physiol Genomics 2009; 39:85–99.
4. Forde N, Spencer TE, Bazer FW, Song G, Roche JF, Lonergan P. Effect of pregnancy and progesterone concentration on expression of genes encoding for transporters or secreted proteins in the bovine endometrium. Physiol Genomics 2010; 41:53–62.
5. Mamo S, Mehta JP, Forde N, McGettigan P, Lonergan P. Conceptus-endometrium crosstalk during maternal recognition of pregnancy in cattle. Biol Reprod 2012; 87:6.
6. Bazer FW, Wu G, Johnson GA, Kim J, Song G. Uterine histotroph and conceptus development: select nutrients and secreted phosphoprotein 1 affect mechanistic target of rapamycin cell signaling in ewes. Biol Reprod 2011; 85:1094–1107.
7. Thatcher WW, Hansen PJ, Gross TS, Helmer SD, Plante C, Bazer FW. Antiluteolytic effects of bovine trophoblast protein-1. J Reprod Fertil Suppl 1989; 37:91–99.
8. Beltman ME, Roche JF, Lonergan P, Forde N, Crowe MA. Evaluation of models to induce low progesterone during the early luteal phase in cattle. Theriogenology 2009; 72:986–992.
9. Clemente M, de La Fuente J, Fair T, Al Naib A, Gutierrez-Adan A, Roche JF, Rizos D, Lonergan P. Progesterone and conceptus elongation in cattle: a direct effect on the embryo or an indirect effect via the endometrium? Reproduction 2009; 138:507–517.
10. Satterfield MC, Bazer FW, Spencer TE. Progesterone regulation of preimplantation conceptus growth and galectin 15 (LGALS15) in the ovine uterus. Biol Reprod 2006; 75:289–296.
11. Vasconcelos JL, Sartori R, Oliveira HN, Guenther JG, Wiltbank MC. Reduction in size of the ovulatory follicle reduces subsequent luteal size and pregnancy rate. Theriogenology 2001; 56:307–314.
12. Sa Filho MF, Crespilho AM, Santos JE, Perry GA, Baruselli PS Ovarian follicle diameter at timed insemination and estrous response influence likelihood of ovulation and pregnancy after estrous synchronization with progesterone or progestin-based protocols in suckled *Bos indicus* cows. Anim Reprod Sci 2010; 120:23–30.
13. Sa Filho MF, Santos JE, Ferreira RM, Sales JN, Baruselli PS Importance of estrus on pregnancy per insemination in suckled *Bos indicus* cows submitted to estradiol/progesterone-based timed insemination protocols. Theriogenology 2011; 76:455–463.
14. Dadarwal D, Mapletoft RJ, Adams GP, Pfeifer LF, Creelman C, Singh J. Effect of progesterone concentration and duration of proestrus on fertility in beef cattle after fixed-time artificial insemination. Theriogenology 2013; 79:859–866.
15. Jinks EM, Smith MF, Atkins JA, Pohler KG, Perry GA, Macneil MD, Roberts AJ, Waterman RC, Alexander LJ, Geary TW. Preovulatory estradiol and the establishment and maintenance of pregnancy in suckled beef cows. J Anim Sci 2013; 91:1176–1185.
16. Miller BG, Moore NW, Murphy L, Stone GM. Early pregnancy in the ewe: effects of oestradiol and progesterone on uterine metabolism and on embryo survival. Aust J Biol Sci 1977; 30:279–288.
17. Bridges GA, Mussard ML, Pate JL, Ott TL, Hansen TR, Day ML. Impact of preovulatory estradiol concentrations on conceptus development and uterine gene expression. Anim Reprod Sci 2012; 133:16–26.
18. Miller BG, Moore NW. Effects of progesterone and oestradiol on endometrial metabolism and embryo survival in the ovariectomized ewe. Theriogenology 1976; 6:636.
19. Miller BG, Moore NW. Effects of progesterone and oestradiol on RNA and protein metabolism in the genital tract and on survival of embryos in the ovariectomized ewe. Aust J Biol Sci 1976; 29:565–573.
20. Mesquita FS, Pugliesi G, Scolari SC, França MR, Ramos RS, Oliveira M, Papa PC, Bressan FF, Meirelles FV, Silva LA, Nogueira GP, Membrive CM, et al. Manipulation of the periovulatory sex steroidal milieu affects endometrial but not luteal gene expression in early diestrus Nelore cows. Theriogenology 2014; 81:861–869.
21. Peres RF, Claro I Jr, Sa Filho OG, Nogueira GP, Vasconcelos JL. Strategies to improve fertility in *Bos indicus* postpubertal heifers and nonlactating cows submitted to fixed-time artificial insemination. Theriogenology 2009; 72:681–689.
22. Garbarino EJ, Hernandez JA, Shearer JK, Risco CA, Thatcher WW. Effect of lameness on ovarian activity in postpartum holstein cows. J Dairy Sci 2004; 87:4123–4131.
23. Siddiqui MA, Gastal EL, Gastal MO, Almamun M, Beg MA, Ginther OJ. Relationship of vascular perfusion of the wall of the preovulatory follicle to in vitro fertilisation and embryo development in heifers. Reproduction 2009; 137:689–697.
24. Langmead B, Salzberg SL. Fast gapped-read alignment with Bowtie 2. Nat Methods 2012; 9:357–359.
25. Li H, Handsaker B, Wysoker A, Fennell T, Ruan J, Homer N, Marth G, Abecasis G, Durbin R; 1000 Genome Project Data Processing Subgroup. The Sequence Alignment/Map format and SAMtools. Bioinformatics 2009; 25:2078–2079.
26. Anders S, Pyl PT, Huber W. HTSeq—a Python framework to work with high-throughput sequencing data. Bioinformatics 2015; 31:166–169.
27. Anders S, Huber W. Differential expression analysis for sequence count data. Genome Biol 2010; 11:R106.
28. Gentleman RC, Carey VJ, Bates DM, Bolstad B, Dettling M, Dudoit S, Ellis B, Gautier L, Ge Y, Gentry J, Hornik K, Hothorn T, et al. Bioconductor: open software development for computational biology and bioinformatics. Genome Biol 2004; 5:R80.
29. Benjamini Y, Hochberg Y. Controlling the false discovery rate: a practical and powerful approach to multiple testing. R Stat Soc Series B Stat Methodol 1995; 57:289–300.
30. Dennis G, Sherman BT, Hosack DA, Yang J, Gao W, Lane HC, Lempicki RA. DAVID: Database for Annotation, Visualization, and Integrated Discovery. Genome Biol 2003; 4:P3.
31. Wheeler DL, Barrett T, Benson DA, Bryant SH, Canese K, Chetvernin V, Church DM, Dicuccio M, Edgar R, Federhen S, Feolo M, Geer LY, et al. Database resources of the National Center for Biotechnology Information. Nucleic Acids Res 2008; 36:D13–21.
32. Carter F, Forde N, Duffy P, Wade M, Fair T, Crowe MA, Evans AC, Kenny DA, Roche JF, Lonergan P. Effect of increasing progesterone concentration from Day 3 of pregnancy on subsequent embryo survival and development in beef heifers. Reprod Fertil Dev 2008; 20:368–375.
33. Bisinotto RS, Ribeiro ES, Lima FS, Martinez N, Greco LF, Barbosa LF, Bueno PP, Scagion LF, Thatcher WW, Santos JE. Targeted progesterone supplementation improves fertility in lactating dairy cows without a corpus luteum at the initiation of the timed artificial insemination protocol. J Dairy Sci 2013; 96:2214–2225.
34. Meneghetti M, Sa Filho OG, Peres RF, Lamb GC, Vasconcelos JL. Fixed-time artificial insemination with estradiol and progesterone for *Bos indicus* cows I: basis for development of protocols. Theriogenology 2009; 72: 179–189.
35. Forde N, Beltman ME, Duffy GB, Duffy P, Mehta JP, O'Gaora P, Roche JF, Lonergan P, Crowe MA. Changes in the endometrial transcriptome during the bovine estrous cycle: effect of low circulating progesterone and consequences for conceptus elongation. Biol Reprod 2011; 84:266–278.
36. Ramos Rdos S, Mesquita FS, D'Alexandri FL, Gonella-Diaza AM, Papa PeC, Binelli M Regulation of the polyamine metabolic pathway in the endometrium of cows during early diestrus. Mol Reprod Dev 2014; 81: 584–594.
37. França MR, Mesquita FS, Lopes E, Pugliesi G, Van Hoeck V, Chiaratti MR, Membrive CB, Papa PC, Binelli M. Modulation of periovulatory endocrine profiles in beef cows: consequences for endometrial glucose transporters and uterine fluid glucose levels. Domest Anim Endocrinol 2014; 50C:83–90.

38. Shimizu T, Krebs S, Bauersachs S, Blum H, Wolf E, Miyamoto A. Actions and interactions of progesterone and estrogen on transcriptome profiles of the bovine endometrium. Physiol Genomics 2010; 42A: 290–300.
39. Forde N, Carter F, Fair T, Crowe MA, Evans AC, Spencer TE, Bazer FW, McBride R, Boland MP, O'Gaora P, Lonergan P, Roche JF. Progesterone-regulated changes in endometrial gene expression contribute to advanced conceptus development in cattle. Biol Reprod 2009; 81:784–794.
40. Ponsuksili S, Murani E, Schwerin M, Schellander K, Tesfaye D, Wimmers K. Gene expression and DNA-methylation of bovine pretransfer endometrium depending on its receptivity after in vitro-produced embryo transfer. PLoS One 2012; 7:e42402.
41. Minten MA, Bilby TR, Bruno RG, Allen CC, Madsen CA, Wang Z, Sawyer JE, Tibary A, Neibergs HL, Geary TW, Bauersachs S, Spencer TE. Effects of fertility on gene expression and function of the bovine endometrium. PLoS One 2013; 8:e69444.
42. Forde N, Mehta JP, Minten M, Crowe MA, Roche JF, Spencer TE, Lonergan P. Effects of low progesterone on the endometrial transcriptome in cattle. Biol Reprod 2012; 87:124.
43. Gao H, Wu G, Spencer TE, Johnson GA, Bazer FW. Select nutrients in the ovine uterine lumen. II. Glucose transporters in the uterus and peri-implantation conceptuses. Biol Reprod 2009; 80:94–104.
44. Killeen AP, Morris DG, Kenny DA, Mullen MP, Diskin MG, Waters SM. Global gene expression in endometrium of high and low fertility heifers during the mid-luteal phase of the estrous cycle. BMC Genomics 2014; 15: 234.
45. Arai M, Yoshioka S, Tasaki Y, Okuda K. Remodeling of bovine endometrium throughout the estrous cycle. Anim Reprod Sci 2013; 142: 1–9.
46. Lonergan P, Woods A, Fair T, Carter F, Rizos D, Ward F, Quinn K, Evans A. Effect of embryo source and recipient progesterone environment on embryo development in cattle. Reprod Fertil Dev 2007; 19:861–868.
47. Mann GE, Fray MD, Lamming GE. Effects of time of progesterone supplementation on embryo development and interferon-tau production in the cow. Vet J 2006; 171:500–503.
48. Wight TN, Kinsella MG, Evanko SP, Potter-Perigo S, Merrilees MJ. Versican and the regulation of cell phenotype in disease. Biochim Biophys Acta 2014; 1840:2441–2451.
49. Zhang G, Ezura Y, Chervoneva I, Robinson PS, Beason DP, Carine ET, Soslowsky LJ, Iozzo RV, Birk DE. Decorin regulates assembly of collagen fibrils and acquisition of biomechanical properties during tendon development. J Cell Biochem 2006; 98:1436–1449.
50. Iozzo RV, Sanderson RD. Proteoglycans in cancer biology, tumour microenvironment and angiogenesis. J Cell Mol Med 2011; 15: 1013–1031.
51. Koohestani F, Braundmeier AG, Mahdian A, Seo J, Bi J, Nowak RA. Extracellular matrix collagen alters cell proliferation and cell cycle progression of human uterine leiomyoma smooth muscle cells. PLoS One 2013; 8:e75844.
52. Ono YJ, Terai Y, Tanabe A, Hayashi A, Hayashi M, Yamashita Y, Kyo S, Ohmichi M. Decorin induced by progesterone plays a crucial role in suppressing endometriosis. J Endocrinol 2014; 223:203–216.
53. Tran KT, Griffith L, Wells A. Extracellular matrix signaling through growth factor receptors during wound healing. Wound Repair Regen 2004; 12:262–268.